Journal of Marine Research, 58, 439–463, 2000

Fortnightly modulation of the estuarine circulation in Juan de Fuca Strait

by Diane Masson[1] **and Patrick F. Cummins**[1]

ABSTRACT

Riverine discharge into the Strait of Georgia sets up a well-defined estuarine circulation within Juan de Fuca Strait, the main path for the freshwater outflow to the continental shelf. At the landward end of Juan de Fuca Strait, the water flows through narrow channels in which strong tidal currents are known to induce significant mixing of the water column, and a spring-neap modulation of the estuarine exchange. A three-dimensional prognostic numerical model has been developed to study the circulation around Vancouver Island, British Columbia. In a series of simulations, the estuarine circulation within Juan de Fuca Strait is established by the Fraser River freshwater discharge. A fortnightly modulation is imposed on the mixing over the various sills to simulate the spring-neap tidal mixing regime. The resulting variation in the estuarine circulation is found to be largely limited to the eastern section of Juan de Fuca Strait, in the vicinity of the sills. Data from current meter moorings and surface salinity data from lighthouse stations compare favorably with the model results.

The effect of local wind forcing on the estuarine exchange is also examined. The model is capable of simulating those rare events during which a concurrence of river freshet, neap tide and northwest wind allows a stronger pulse of fresh surface water to escape relatively unmixed into the eastern end of Juan de Fuca Strait. The disturbance then propagates along the northern shore of the strait as a first mode internal Kelvin wave. Finally, the effect of the fortnightly modulation on the export of freshwater onto the continental shelf is examined. It is found that small amplitude coastal trapped waves are generated near the mouth of Juan de Fuca. However, this fortnightly signal is weak in comparison to the energetic wind-induced variations typically found over the shelf.

1. Introduction

On the southern coast of British Columbia, the Fraser River discharges a substantial amount of freshwater into the Strait of Georgia, a large semi-enclosed basin (see Fig. 1). Most of this freshwater reaches the continental shelf through Juan de Fuca Strait, a long weakly stratified, partially mixed estuary with strong tidal currents. Over the shelf, the buoyancy outflow drives a coastal current flowing poleward along Vancouver Island, with its origin near the mouth of the strait (e.g. Thomson *et al.,* 1989; Masson and Cummins, 1999). The flow in Juan de Fuca Strait undergoes a strong seasonal cycle as the Fraser River discharge varies from a low winter rate to a peak discharge in early summer resulting

1. Institute of Ocean Sciences, P.O. Box 6000, Sidney, British Columbia, Canada V8L 4B2. ***email: massond@dfo-mpo.gc.ca***

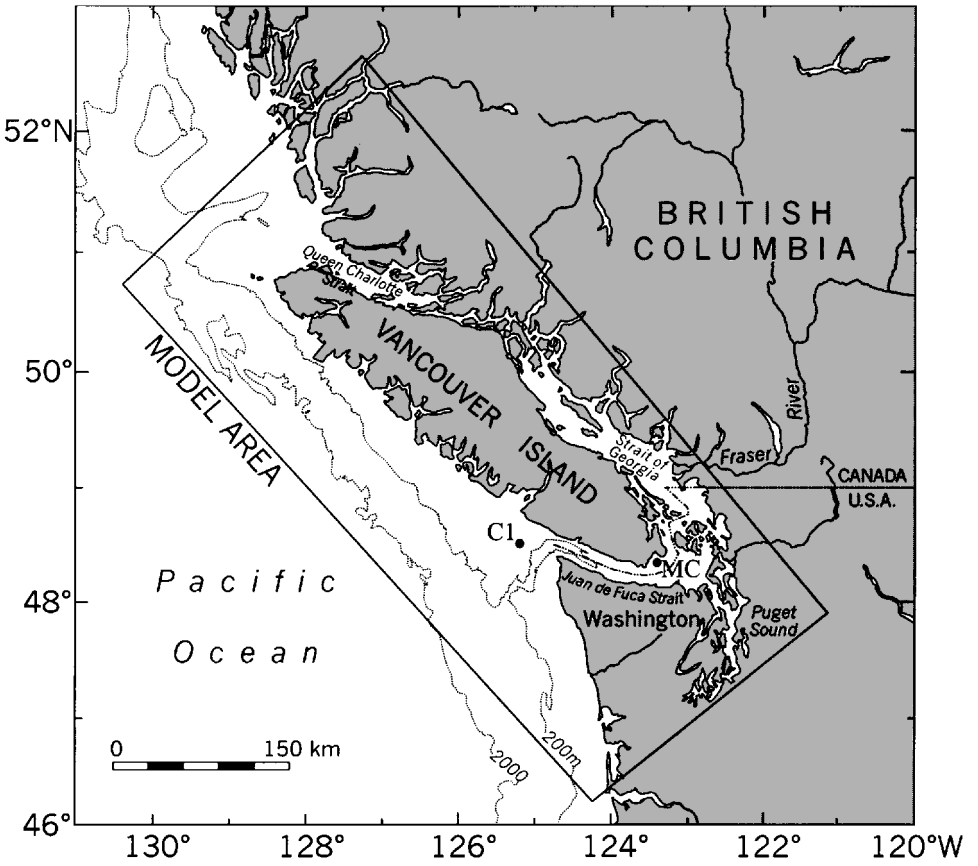

Figure 1. The Vancouver Island coastal area and the region encompassed by the numerical model. Also included are the positions of two current meter moorings, C1 and MC, mentioned in Section 5.

from snow melt. The estuarine exchange of water is also subject to tidally induced mixing over a series of shallow sills located in the eastern end of the strait. As the succession of spring and neap tides modulates the mixing over the sills, it is believed that it will also regulate the estuarine exchange (e.g. Griffin and LeBlond, 1990).

Holbrook *et al.* (1980) found that the circulation within Juan de Fuca Strait was mostly influenced by coastal winds, with reversals of the estuarine flow associated with strong southerly coastal winds. However, most of their data were collected during the winter months when the estuarine circulation is relatively weak and the coastal downwelling winds are more favorable to reversals. Although such reversals are occasionally observed in summer (Frisch *et al.,* 1981), they are uncommon, and mean flows within the strait are expected to be driven mainly by the freshwater runoff.

In an early investigation, Herlinveaux and Tully (1961) give an overall description of the

water properties and currents found in Juan de Fuca Strait. They identify tidal mixing over shallow sills as an important mechanism in determining the general water properties inside the strait. The surface outflow is mixed with the deeper return flow as it travels seaward over the sill at Boundary Pass, and the waters of the deep return flow are also mixed with the upper outflow as they advance landward over Victoria Sill (depicted in Fig. 2). Accordingly, Herlinveaux and Tully (1961) divide Juan de Fuca Strait into an inner and outer region separated by Victoria Sill, with weaker stratification within the inner strait. They also mention that near-surface water properties follow a fortnightly cycle similar to the variation in tidal speeds, with higher surface salinity during periods of maximum tidal flow. Geyer and Cannon (1982) identified a link between fortnightly variations in tidal mixing over the sill at the entrance of Puget Sound (Fig. 2) and the penetration of saltier ocean water at depth. The role of tidal mixing in controlling the estuarine circulation in Juan de Fuca Strait was examined in greater detail by Griffin and LeBlond (1990). Using surface salinity data collected at lighthouse stations, they identified lower salinity values at Race Rocks (located on the northern shore of the eastern part of the strait—see Fig. 2), during periods of neap tides. They also found that the lowest surface salinity values were measured during freshet, at neap tides that were coincident with northwesterly winds over the Strait of Georgia.

The effect of the variations in buoyancy forcing within Juan de Fuca Strait on the shelf dynamics was examined by Hickey *et al.* (1991). In an attempt to identify signals specifically associated with buoyant outflow from the strait, they deployed an extensive array of current meters across the mouth of Juan de Fuca Strait and over the shelf. Their results show that, during summer, variability over the shelf is dominated by wind-driven motions and, consequently, it was not possible to identify clearly the effects of buoyancy-driven variations.

LeBlond *et al.* (1994) constructed a two-layer box-model with plausible but essentially ad hoc parameterizations to simulate salinity variations in Juan de Fuca Strait. They were able to reproduce the surface salinity signal at Race Rocks for many observed events caused by the fortnightly mixing and a northwesterly wind. Although their model had some success in simulating surface salinity variations in the eastern strait, they found that water property changes measured near the mouth of the strait were largely determined by other causes. In fact, no detectable link was found between variations occurring at the two ends of Juan de Fuca Strait.

The works cited above have clearly established that the fortnightly modulations of mixing over the sills have a marked influence on the properties of the surface waters in the eastern section of Juan de Fuca Strait. However, an important question yet to be addressed is how significant this modulation is in terms of influencing the downstream coastal circulation within the Strait of Juan de Fuca and over the continental shelf. In other words, is this a local phenomenon significantly affecting the surface waters only around the sills where the intense tidally induced mixing occurs, or is the export of freshwater onto the shelf strongly regulated by this mixing?

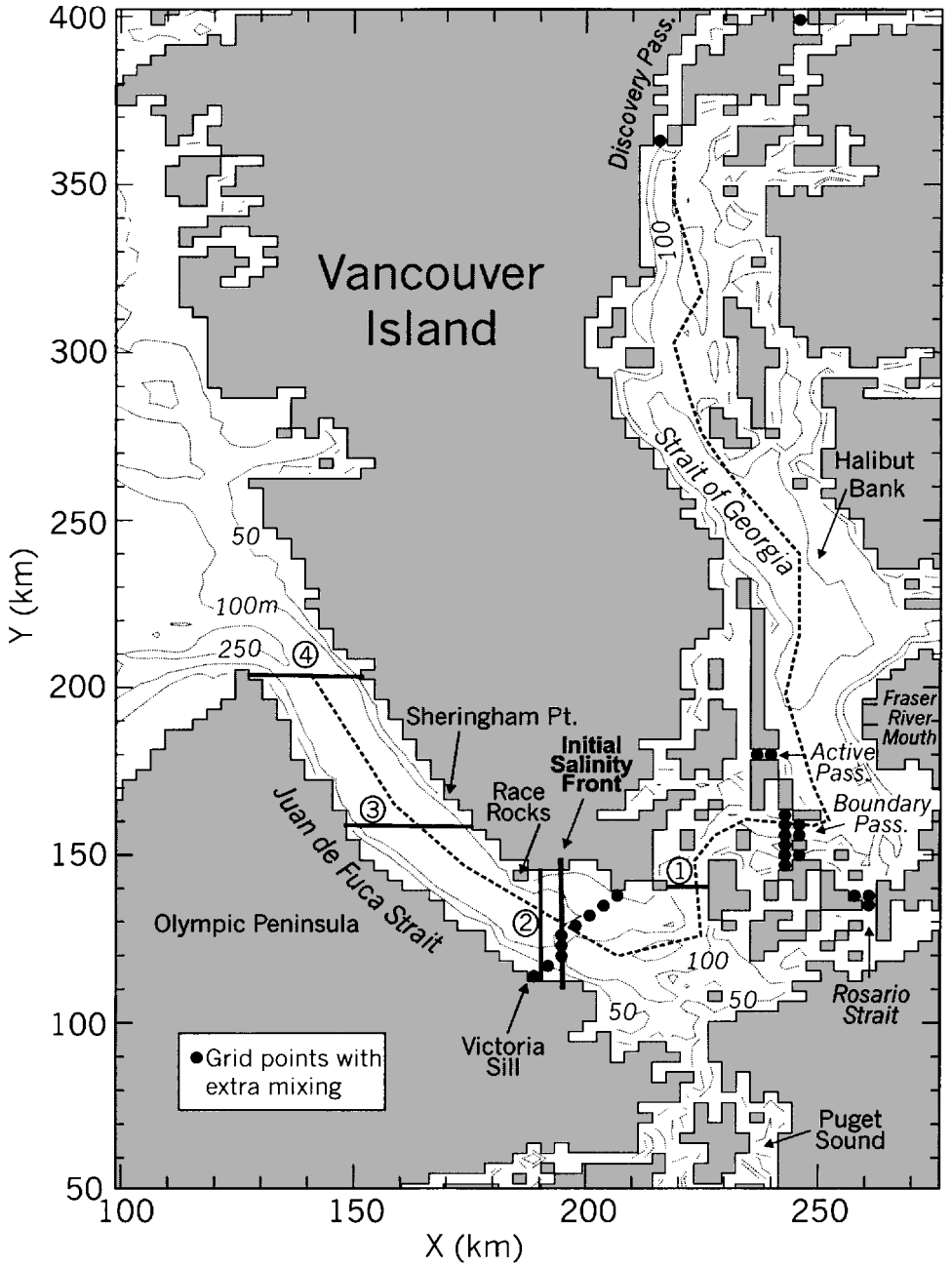

Figure 2. Details of the numerical grid for the Strait of Georgia and Juan de Fuca Strait. The numbers 1 to 4 refer to cross-sections of the estuary used in the analysis. Black circles indicate grid points with additional vertical mixing.

In this paper, we focus on the summer period when the buoyancy flux is maximum and the estuarine circulation it establishes is the strongest. In particular, the role of tidally-induced fortnightly mixing of the estuarine circulation, along with the effect of the wind stress, in the formation of freshwater pulses in Juan de Fuca Strait is examined using numerical results and field data. To this end, we present a series of numerical simulations with the Princeton Ocean Model (POM), as well as a comparison of results with data collected in Juan de Fuca Strait and on the shelf. In the next section, the numerical model is briefly described. This is followed by an analysis of the fortnightly modulation of the estuarine circulation within Juan de Fuca Strait. The effects of wind stress over the Strait of Georgia on the formation of stronger freshwater pulses are then examined. Finally, the influence of buoyancy variations at the mouth of the estuary on the shelf dynamics is discussed. The final section summarizes and gives conclusions.

2. Numerical model

For this study, we use the Princeton Ocean Model (POM), a three-dimensional primitive equation model initially developed by Blumberg and Mellor (1987). The model solves the time-dependent, primitive equations of motion in a bottom-following sigma-coordinate system. It contains a free surface formulation and complete thermodynamics, with an embedded level—2.5 turbulence closure submodel to provide vertical mixing coefficients (Mellor and Yamada, 1982). A staggered C-grid differencing scheme is adopted with explicit time stepping, except for the vertical diffusion terms which are treated implicitly. The model uses a mode-splitting method, with a short external mode time step and a longer three-dimensional internal time step, based on the external and internal CFL conditions, respectively. The horizontal viscosity and diffusivity are parameterized by the standard Smagorinsky formula. The present version of the model includes modifications made by Oey and Chen (1992) and Oey (1996) to include riverine discharge.

The model domain represents the coastal waters surrounding Vancouver Island including: the Strait of Georgia, Juan de Fuca Strait and Puget Sound, the continental shelf off the west coast of Vancouver Island, and, finally, Queen Charlotte and Johnstone straits to the north (Fig. 1). The grid resolution is 3 km and there are 15 sigma levels in the vertical. A clockwise rotation of 40° from True North is applied to align approximately the local coastline with the y-coordinate of the model. The model was also run with a 1.5 km grid and with 31 sigma levels to test for resolution effects, with essentially similar results. The western and northern sides of the domain are treated as open boundaries with radiation conditions combined with a sponge layer to minimize unwanted reflections at the boundary. A similar model configuration was used by Masson and Cummins (1999) to examine the formation of the Vancouver Island Coastal Current by the buoyancy flux out of the mouth of Juan de Fuca. The model successfully represented the estuarine flow at the mouth of the estuary as well as the structure and strength of the coastal current. In the present application, we turn our attention to the variability of the circulation within the estuary itself.

In these coastal waters, variations in water density are determined largely by the salinity field. Therefore, for simplicity, the temperature of the ocean and of the freshwater discharge is fixed at $T = 8°C$. Since temperature is constant, the temperature equation is not solved and density variations are controlled by salinity alone. As mentioned above, during summer, water properties in Juan de Fuca Strait are strongly influenced by the Fraser River plume and by the intense tidally-induced mixing occurring over the various shallow sills. In Figure 3a, salinity contours are given for a vertical section located on the along-strait track indicated in Figure 2 as a dashed line. The section extends from the mouth of Juan de Fuca to the northern end of the Strait of Georgia and is based on data collected in early July, 1968 (Crean and Ages, 1971). It shows typical summer conditions, including (1) the shallow surface plume near the mouth of the Fraser River with a strong front located above the sill at Boundary Pass, (2) a saltier deep return flow with an associated salinity front above Victoria sill, and (3) a salinity contrast of about 3 psu between the deep waters over the shelf and those inside the Strait of Georgia. Because the fortnightly modulations represent a perturbation upon this basic state, our first objective was to reproduce accurately the main features of the salinity field inside the estuary.

To simulate realistic summer conditions, it is necessary to represent the salinity contrast between the subsurface waters of the interior basins and the waters on the shelf, in addition to including the Fraser River discharge. This could be achieved by forcing an initially uniform ocean by the river discharge on a long enough time scale (several years) to allow the water within the interior basin to reach low enough salinity values. Such an approach was used by Masson and Cummins (1999) and found, after very long integrations, to tend to produce a realistic mean state. Since such long integration times are impractical and, because the present objective is not to derive a realistic mean state but rather to study variations on that mean state, a more rapid initialization technique was chosen. The model is initialized in a dam-breaking configuration with an oceanic salinity of 33.8 psu and an initial salinity of 30 psu within the estuary. The location of the initial salinity front is indicated on Figure 2. At time $t \geq 0$, the dam breaks and the freshwater of the estuary is allowed to spread over, and mix with, the saline ocean water. Such an approach is not uncommon for modeling estuarine systems and may lead, after an adjustment period, to realistic conditions (e.g. Oey and Mellor, 1993).

The Fraser River water enters the Strait of Georgia through two channels, with about 87% of the total discharge in the northern arm. Accordingly, as in Masson and Cummins (1999), the river is modeled as two neighboring point sources of freshwater (see Fig. 2), with most of the discharge out of the northern point. The freshwater is introduced in the continuity equation as a surface volume flux of zero salinity water (Oey, 1996). The discharge rate is held constant at 5400 $m^3\ s^{-1}$, a relatively large value representative of early summer freshet conditions.

As the tide goes through its fortnightly cycle of neap and spring periods, the mixing over the sills follows a similar pattern. To introduce this time varying forcing, without having to introduce the complexity of the tidal flow itself, tidal mixing over the sills is parameterized

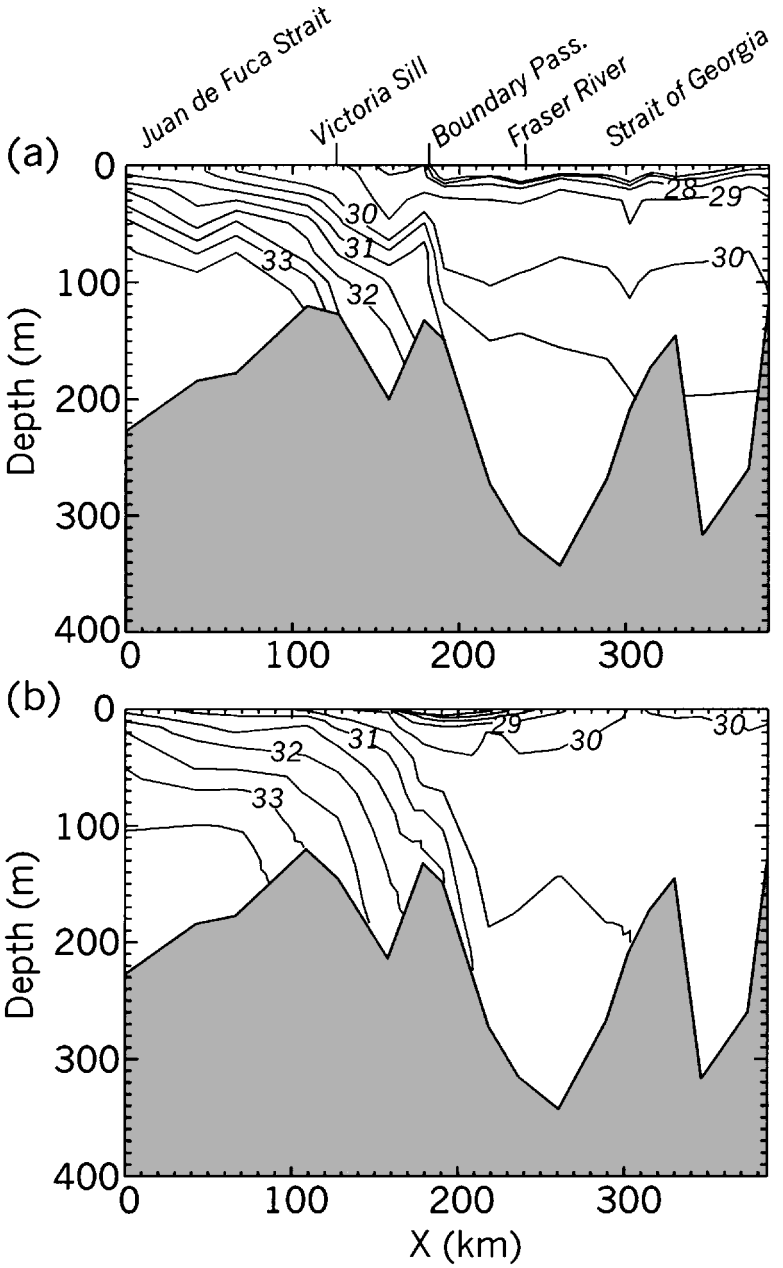

Figure 3. Salinity contours along a transect through the Straits of Georgia and Juan de Fuca, (a) as measured on 1–6 July 1968 (from Crean and Ages, 1971), and (b) as given by the numerical results of the basic experiment. In (b), the salinity field is a 5-day average for the integration period ending at day 40.

simply by imposing a fortnightly time variation on the vertical mixing coefficients. This approach is also motivated by the fact that the strong mixing over the sills is known to be associated with small-scale hydraulic phenomena (Farmer and Smith, 1980) which may not be readily represented in the model, even with the tide included. Over the sills, the value of the vertical viscosity and diffusivity coefficients, K_M and K_H, is given by

$$K_{M/H}(t) = K'_{M/H}(t) + \frac{a}{2}[1 + \sin(\sigma t)] \tag{1}$$

where $K'_{M/H}(t)$ takes the standard values given by the turbulence closure scheme, a is a constant, and σ the fortnightly frequency. Geyer and Cannon (1982) first proposed a similar approach in their study of deep water renewal in Puget Sound. From observations taken in Admiralty Inlet, they found that, over the sill, the eddy coefficients appear to have values of the order of 0.1 $m^2\ s^{-1}$, and that they must vary in time by a factor of two. Such a parameterization was also used by Hibiya *et al.* (1998) in a study of the effect of fortnightly modulated mixing over a sill on the circulation of an idealized two-dimensional estuary. They found that a high resolution nonhydrostatic numerical model that included the tide explicitly gave results similar to those produced by modeling tidal mixing simply as a fortnightly modulation of the vertical mixing coefficients above the sill. Accordingly, the time varying mixing is added over regions of the model where a shallow sill is present, and where it is known that vigorous tidal mixing occurs: Victoria sill, Boundary Pass, Active Pass, Rosario Strait, and Discovery Passage (see Fig. 2). At these locations, the vertical mixing coefficients are modified according to (1), with $a = 0.08\ m^2\ s^{-1}$. To test the sensitivity of the results on the mixing intensity, the experiment was repeated with values of $a = 0.8\ m^2\ s^{-1}$ and $a = 0.008\ m^2\ s^{-1}$. Although the specific locations of the model points within the areas of intense mixing are somewhat arbitrary, we based our choice on (1) knowledge of the general nature of the estuarine circulation as depicted in Figure 3a, in particular on the position of the surface and deep flow salinity fronts, and (2) on the available information on the locations of vigorous vertical mixing due to large tidal currents (e.g., Foreman *et al.,* 1995).

By restricting the effect of the tides to a modulated mixing coefficient in the sill areas, some aspects of the tidally induced circulation in the estuary may not be included in the model simulations. For example, the possible effect of tidal pumping on the dynamics of the flow over the sill is not represented. Tidal pumping can have a local importance on the salt flux balance, especially near lateral constrictions and sills (e.g. Geyer and Nepf, 1996). However, since the transport in each layer must be nearly continuous along the estuary, large local values of tidal pumping must be associated with local variations in the Eulerian salt flux. Thus, as pointed out by Geyer and Nepf (1996), tidal pumping is often only of local significance to the overall salt balance in partially mixed estuaries, and the estuarine salt flux is the dominant contributor to the overall upstream salt transport. Consequently, the present results should capture the dominant processes that determine the overall

characteristics of the problem studied here which is the effect of the fortnightly modulated mixing on the estuarine circulation downstream from the sill areas.

For some of the experiments, the model is also forced by a pulse-like wind stress applied over the Strait of Georgia. As is typical of the area in summer, the wind is assumed to blow toward the southeast, along the *y*-axis of the model, with a peak amplitude varying between 2 and 8 dyne cm^{-2}.

3. Fortnightly modulation inside the estuary

Most of the results discussed below are obtained from a basic case, referred to as Exp. A. In this numerical experiment, the model is initialized in a dam-breaking configuration as described in the previous section. The water in the interior basin is fresher (30 psu) than the ocean water (33.8 psu), with the transition located in the eastern Juan de Fuca Strait (see Fig. 2). Within each water mass, there is no initial vertical stratification. The river discharge is started at the beginning of the experiment with a constant flux of 5400 m^3 s^{-1}. The fortnightly modulation of the mixing is also included from the outset, following Eq. (1).

After a period of rapid adjustment to the initial shock of the breaking dam, which lasts for about 30 days, the coastal system attains a quasi-steady state with much slower variations. For the numerical simulations to be realistic, conditions inside the estuary should approach, at the end of this adjustment period, typical conditions prevalent in the Georgia-Juan de Fuca system during the summer freshet. Figure 3b shows a 5-day average of the salinity field, along the same section as Figure 3a, for the period ending on day 40 of the integration. The comparison of Figures 3a and 3b indicates that the main features of the observed structure of the water column are represented in the model: the plume originating at the river mouth and spreading over the Strait of Georgia, the surface front in Boundary Pass, and the deep front above Victoria Sill. Although the location of the front of the river plume is well represented, the observed plume extends somewhat farther to the north over the Strait of Georgia. A longer time would appear to be required for the model to accumulate sufficient fresh river water in the top layer of the strait. However, this discrepancy should not be significant for this process study.

The initialization of the model should also allow a realistic estuarine circulation to develop within Juan de Fuca Strait. On Figure 4, contours of the component of velocity normal to a cross-section located midway along Juan de Fuca Strait (Section 3 on Fig. 2) are compared with observations from a similar section obtained during summer, 1975 (Labrecque *et al.,* 1994). In both cases, the velocities are an average over 40 days; from 26 May to 15 July for the current meter data, and from day 50–90 for the model. The simulated currents are of comparable magnitude to observations and reproduce well some of the main features of the along-strait circulation: (1) stronger surface outflow away from the sides, (2) maximum velocities on the south side of the channel for the two layers, and, finally, (3) the zero long-strait velocity at a depth of about 70 to 90 m.

We now examine the fortnightly modulation of the water properties inside the estuary both for the fresh upper-layer outflow and the deeper return flow. Surface salinity data have

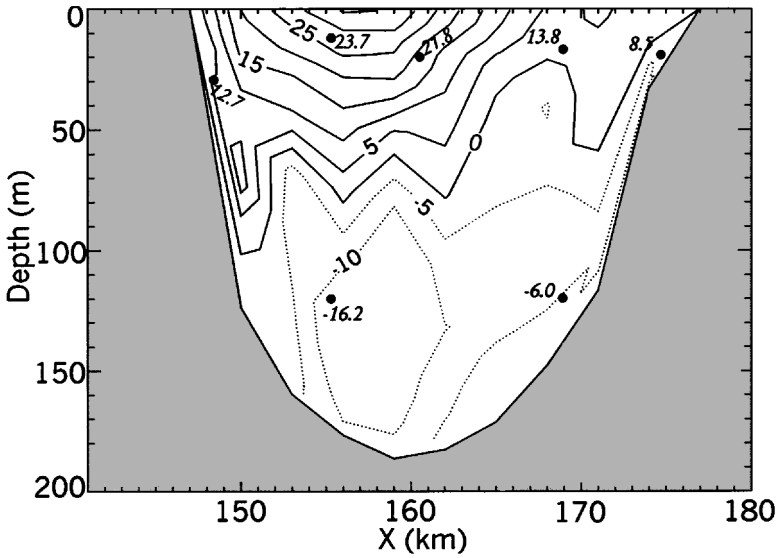

Figure 4. Contours of the velocity component normal to a section located midway along Juan de Fuca Strait (section 3 of Fig. 2), averaged over 40 days of the basic experiment (day 50–90). Also included are mean summer currents measured with current meters on a similar section in 1975 (from Labrecque *et al.,* 1994).

been collected daily at the Race Rocks Lighthouse station since 1936 (see Fig. 2 for location). LeBlond *et al.* (1994) used this data set to tune and validate their box model which, in most cases, was able to reproduce the marked fortnightly surface salinity signal measured at this location. In Figure 5, a 50-day segment of the long Race Rocks data set (Fig. 5a) is compared with surface salinity from a nearby model point (Fig. 5b). The measurements are taken from the summer of 1969, and are quite representative of seasonal conditions during periods of relatively light winds. Also given in the figure is the cube of the tidal velocities at Boundary Pass, and the additional mixing in the model simulations (as per Eq. 1). The tidal velocities of Figure 5a were calculated with the three-dimensional barotropic, finite element tidal model of Foreman *et al.* (1995). The cube of the velocities is used here as an index of the rate of tidal energy dissipation and mixing (e.g. Griffin and LeBlond, 1990). It is clear that the model reproduces the correct mean surface salinity around Race Rocks (about 31 psu), as well as a realistic spring-neap oscillation of the surface salinity, both in magnitude (about 1 psu) and in phase relative to the tidal currents. In both the model and the data, a period of energetic spring tides is followed by higher values of surface salinity, while weaker neap tides allow a fresher surface outflow, with a phase lag of about 2 days at Race Rocks.

In addition to modulating the surface water properties in eastern Juan de Fuca, the fortnightly mixing also affects the waters of the deeper return flow. Figure 6a presents salinity and tidal current data collected from a current meter deployed during the summer

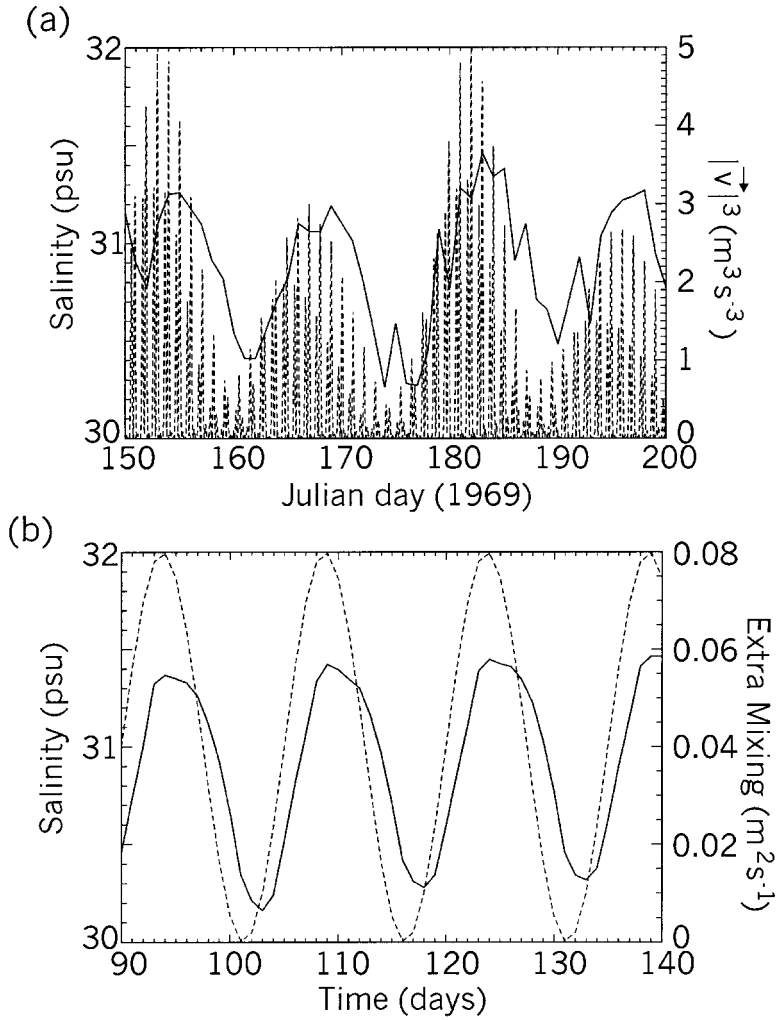

Figure 5. Surface salinity and tidal mixing near Race Rocks from (a) measurements and (b) the basic numerical experiment.

of 1989, near the bottom (80 m depth), over Victoria Sill (Birch, 1991). Following periods of intense tidal mixing, the saline return flow is diluted with water from the fresh surface outflow, resulting in a fortnightly modulation of the salinity at depth that is similar to, but weaker (with an amplitude of about 0.5 psu), than the surface signal identified near Race Rocks. In the next figure (6b), salinity near the bottom is given for a model point located over Victoria sill, along with the extra vertical mixing. Again, the model results show a mean salinity (33 psu) and a modulation amplitude (0.7 psu) that is comparable to the measurements. However, contrary to the results for the surface salinity, there is a difference between the phase of the modeled and measured signal. The current meter data indicate

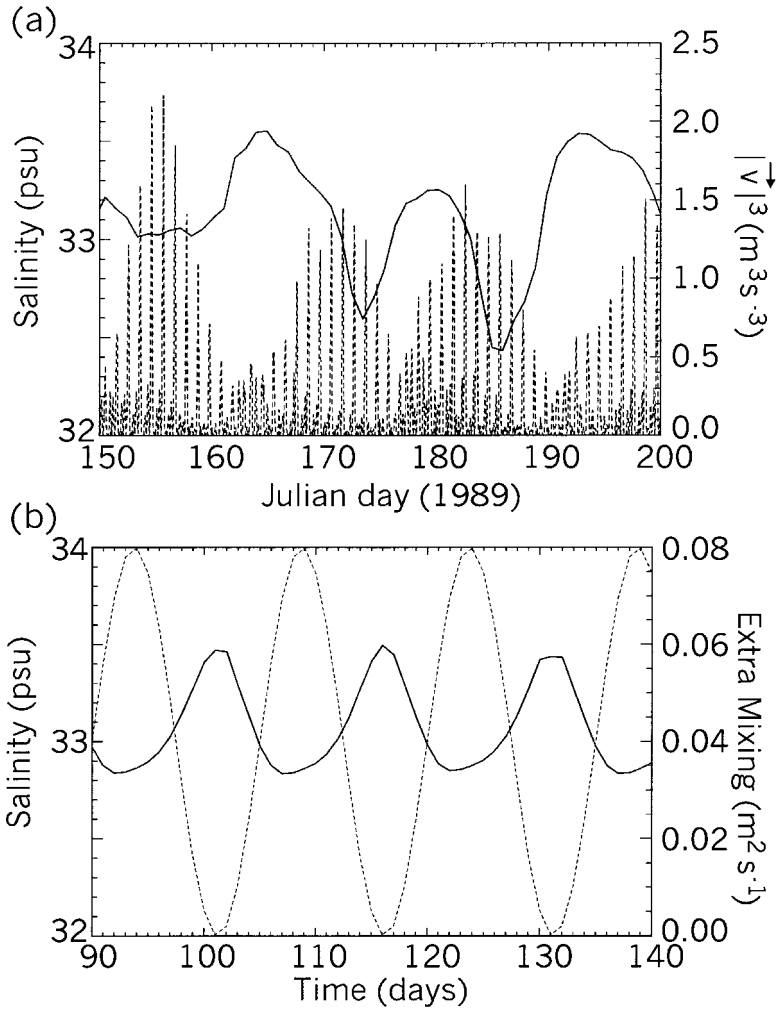

Figure 6. Near-bottom salinity (solid line) and tidal mixing (dashed line) over Victoria Sill from (a) measurements and (b) the basic experiment.

that the salinity signal follows the mixing intensity by a few days whereas the model shows a nearly instantaneous response. One possible reason for this discrepancy is that the model does not explicitly include tidal currents. Generally, there are two distinct local processes associated with the tides. The first is a fortnightly modulation of the local mixing as parameterized by (1) and included in the model. The second is a variation of the water properties caused by the varying tidal currents over the sill (such as the one associated with tidal pumping), with a tidal excursion of about 10 to 15 km (e.g. Herlinveaux and Tully, 1961). Because the main front of the surface plume is well up-stream from Race Rocks, local tidal currents have little or no influence on the salinity signal there. On the other hand,

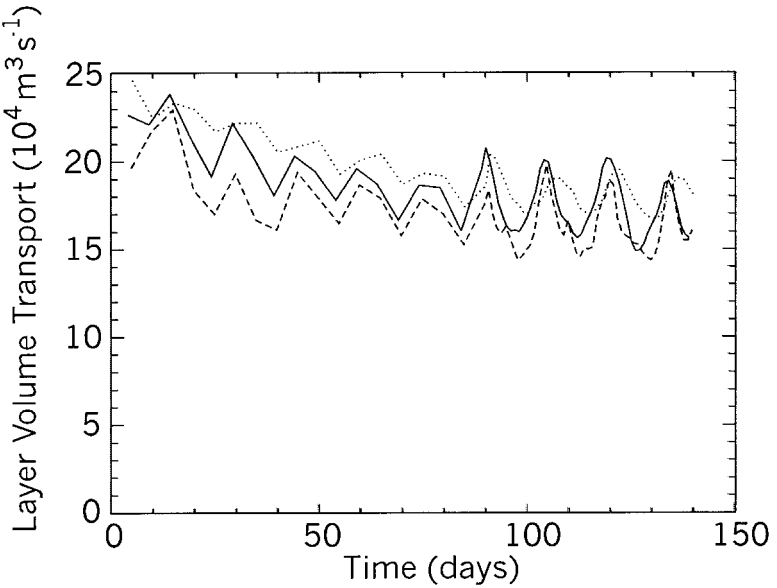

Figure 7. Layer volume transport across a section midway along Juan de Fuca Strait (section 3 of Fig. 2). Results of the basic experiment, with the mixing coefficient $a = 0.08$ m^2 s^{-1} are given by the solid line. Also included are results of experiments with reduced mixing, $a = 0.008$ m^2 s^{-1}, (dotted line), and increased mixing, $a = 0.8$ m^2 s^{-1}, (dashed line).

the main front of the deep return flow is directly over Victoria Sill, as this is the first shallow region encountered on its landward path (Herlinveaux and Tully, 1961). Therefore, effects due directly to the tidal currents may be expected to have some influence on the measured salinity of Figure 6a.

The results presented above established that local water properties in the region of large tidally induced mixing follow a marked fortnightly modulation. How important is the modulation of the vertical mixing due to tides for the overall estuarine system? Griffin and LeBlond (1990) suggested that the spring-neap tidal mixing produces a large-scale density tide within Juan de Fuca Strait which strongly modulates the export of freshwater onto the continental shelf, and therefore the buoyancy forcing of the coastal current. In their view, mixing over the shallow sills acts like a barrier because the local intense vertical exchange of momentum could, at times, completely overwhelm the sheared estuarine flow. LeBlond *et al.* (1994) further examined the idea of a leaky gate controlling the export of freshwater in Juan de Fuca Strait, but found that conditions at the western end of the strait are subject to other influences, and so did not support this hypothesis. Recently, Pawlowicz and Farmer (1998) examined the same problem, using a kinematic theory applied to a simple two-layer model. Their analysis also shows little evidence of a strong spring/neap modulation in the layer transport within Juan de Fuca.

The modeled volume transport of the surface layer is presented in Figure 7 for the basic

experiment along with the results of the experiments where the mixing coefficient, a, is increased or decreased by a factor of 10. This is the transport computed for a cross-section located midway along Juan de Fuca Strait (Section 3 of Fig. 2). After the initial adjustment period of about 30 days, the volume transport assumes values between 1.5 and 2.0 $\times$ 10^5 m^3 s^{-1}. These values of transport are in general agreement with previous transport estimates obtained from current meter data collected on cross-channel sections also located midway along Juan de Fuca Strait. For example, the layer volume transport during spring 1973 was estimated by Godin *et al.* (1981) to vary between 0.9 and 1.6 $\times$ 10^5 m^3 s^{-1}, for a pre-freshet discharge rate of about 3000 m^3s^{-1}. Similarly, Labrecque *et al.* (1994) estimated a transport of 2.5 $\times$ 10^5 m^3 s^{-1} over a summer period in 1975 when the discharge rate was about 6000 m^3s^{-1}.

Also evident in Figure 7 is that, for the three experiments, the transport includes a fortnightly component, with smaller transport values following periods of more intense mixing, with a time lag of about 2 days. This result is consistent with arguments given in Park and Kuo (1996) that, for large estuaries, the fortnightly varying vertical mixing should lead to a decrease in residual circulation following spring tides. They identify two main effects of varying vertical mixing on the estuarine transport: the direct effect of weakening the circulation by enhanced vertical momentum exchange, and the indirect opposing effect of strengthening the circulation by increasing the longitudinal salinity gradient. In large estuaries like the one studied here, the spring-neap cycle is short compared to the response time of the longitudinal salinity distribution, hence the former direct effect dominates.

Although the estuarine transport of Figure 7 displays a clear fortnightly modulation, it is of relatively modest amplitude (about 20% of the mean), and at no time is it strong enough to arrest the estuarine transport. It should not be surprising to see the limited extent of the influence of the mixing on the estuarine circulation, as the main driving force for the outflow, the along-strait barotropic pressure gradient caused by the hydraulic head formed near the mouth of the river is always present. It is also worth noting that these results show only a weak sensitivity to large variations in the mixing intensity in the sill areas. Overall, these results indicate that, although the locally intense mixing over the sills modulates the estuarine exchange, it does not strongly control the overall characteristics of the estuarine circulation.

To better visualize the locality of the spring/neap modulations, the results of harmonic analysis of the surface salinity are given in Figure 8. The figure gives the amplitude and the phase of the 15 day signal for the salinity along the uppermost sigma level of the model, for a 40 day period starting on day 100. Large values (greater than 0.5 psu) are found close to the intense mixing area in the southern Strait of Georgia and over Victoria Sill. However, the fortnightly signal is rapidly attenuated as it propagates seaward in Juan de Fuca Strait and is less than 0.25 psu at the mouth. These results are also in agreement with data presented in Griffin and LeBlond (1990), which show that the fortnightly signal of the surface salinity measured at Sheringham Point, 30 km seaward of Race Rocks, is significantly smaller than the one observed at Race Rocks, with a phase lag of close to 40°

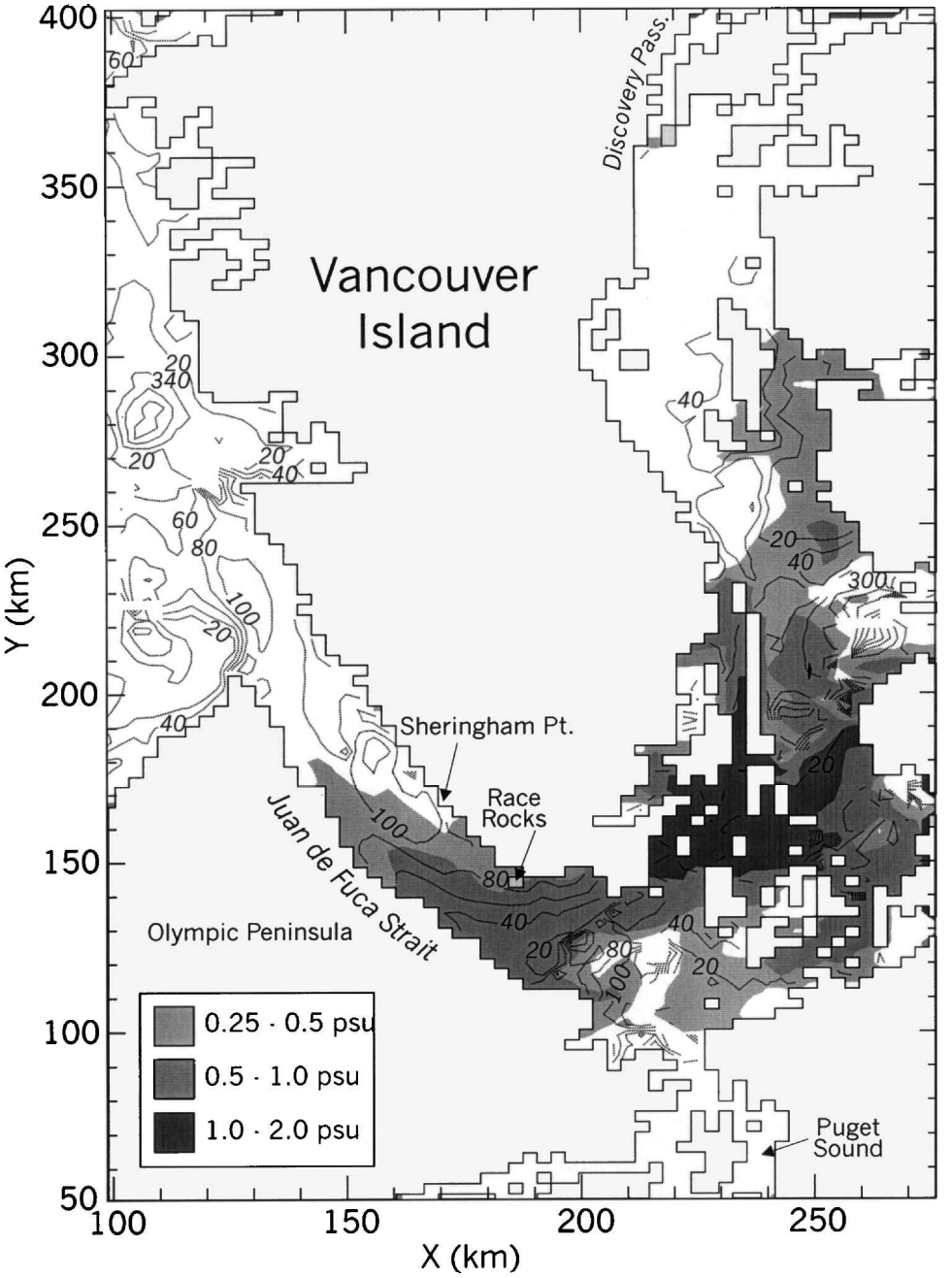

Figure 8. Amplitude and phase of the fortnightly signal of the surface salinity. The harmonic analysis is done on a 40-day period starting at day 100 of the basic experiment.

(see Fig. 2 for location). It is thus evident that the model results support the idea that the fortnightly modulations are important mainly in the vicinity of the intense tidal mixing area, with rapidly diminishing influence downstream.

The limitation of the strong 15-day signal to the area located in between the two mixing areas can be explained by the 'two-door effect.' Referring to Figure 5, it is clear that the time window during which a surface pulse of freshwater can propagate downstream of Boundary Pass (the first door) before being mixed is quite narrow (a few days during minimum neap tide). By the time a fresh pulse of surface water reaches the next mixing region above Victoria Sill (the second door), the tidal intensity has already increased and the surface waters are mixed with the underlying saltier return flow. The two-door effect is thus efficient in confining the fortnightly signal to the eastern side of Juan de Fuca Strait.

4. Wind-induced freshwater pulses

While the model can reproduce the regular tidally induced fortnightly modulation of the water properties observed in eastern Juan de Fuca Strait, the 51-year long (1937–1998) salinity record measured at Race Rocks is punctuated by more dramatic events, with salinity values dropping by as much as 2 psu, to values as low as 28 psu. These extreme events are not common; a careful examination of the record reveals only 50 summer occurrences (June to September), with salinity values decreasing by close to 2 psu from the seasonal mean for several days, an average of about one event per year.

Griffin and LeBlond (1990) found that these strong freshwater pulses occur during summer neap periods when a northwest wind blows over the Strait of Georgia. Assuming that tidal mixing over the sills is related to some kind of hydraulic control mechanism for the estuarine flow, they characterize the effect by defining an internal Froude number $F_i = u/c_i$, where u is the depth-averaged ebb tidal velocity, and c_i the local phase speed of long interfacial waves at Boundary Pass. For most of the extreme freshwater events, their estimate of F_i is smaller than unity, implying subcritical conditions over the sill, with the fresh surface outflow being allowed to flow seaward relatively unmixed. These small values of the Froude number arise when small neap tidal velocities are concurrent with larger internal wave speeds. The latter are the consequence of stronger stratification found at the entrance of Boundary Pass as the river plume is forced to the southern reaches of the Strait of Georgia by a northwesterly wind. Thus, they conclude that for strong freshwater pulses to penetrate into eastern Juan de Fuca Strait, these three necessary conditions must be met: a strong river discharge (typical of the summer period), low neap tidal velocities, and a northwest wind blowing over the Strait of Georgia.

To test this hypothesis, the model is run by adding to the basic experiment described above a northwesterly wind pulse blowing over the Strait of Georgia. The northwesterly wind stress is applied along the negative y-axis, over the Strait of Georgia region only, on an area delimited by 165 km $\leq y \leq$ 400 km and 200 km $\leq x \leq$ 300 km (see Fig. 2). The influence of the local wind blowing over Juan de Fuca Strait is presumed to be of less importance because of the thicker surface layer there. To simulate a typical summer wind

event, the amplitude of the wind stress is determined by a prescribed Gaussian-shaped pulse, with values increasing from 0 to 4 dyne cm^{-2} over about 10 days. Initial conditions are taken as those conditions on day 120 of the basic experiment, and the model is then run for an additional 30 days. The wind stress thus reaches a maximum amplitude on the following neap tide, on day 131 (Fig. 9b). The along-strait wind is very efficient in forcing the surface river plume toward the southern shores of the Strait of Georgia, bringing more freshwater near the entrance to the passes leading to Juan de Fuca Strait. A similar behavior for the plume was observed by Royer and Emery (1985) who found the plume movement consistent with wind-driven advection.

As the time of minimum mixing in Boundary Pass is approached, the increased barotropic pressure gradient due to the wind-induced sea level rise in the southern Strait of Georgia forces a large amount of freshwater to escape through Haro Strait as a gravity current. The modeled freshwater pulse then moves seaward into eastern Juan de Fuca Strait. Associated with this pulse is an increased sea level height, increased upper layer transport, lower surface salinity, and increased seaward velocities in the upper layer.

The surface salinity during two such freshwater events measured at Race Rocks is given in Figure 9c, for the summers of 1984 (an event documented by Hickey *et al.,* 1991) and of 1997. In each case, a period of 40 days is shown, starting on June 30 and July 19 for 1984 and 1997, respectively. For both events, the freshwater pulse is associated with a neap tide during which time there was a strong northwesterly wind pulse over the Strait of Georgia. Figure 9a illustrates the wind stress over the Strait of Georgia, as measured over Halibut Bank near the middle of the strait (Fig. 2), and the tidal mixing index, based on the model of Foreman *et al.* (1995), for the 1997 event. A similar situation occurred in 1984 as well. For both events, the measured salinity follows a similar pattern, with a decrease of about 2 psu lasting for a few days. There is, however, a marked difference in the background salinity value for the two cases, with a lower overall salinity for the 1997 case. This change in the mean properties is likely due to the extraordinarily large river discharge that occurred in 1997 (an annual average of the daily discharge rate of 3687 $m^3\ s^{-1}$). In contrast, the average discharge rate for 1984 of 2727 $m^3\ s^{-1}$ was closer to the long term mean.

The surface salinity obtained from the model grid point corresponding to the Race Rocks location is given in Figure 9d. A clear pulse of freshwater reaches the area, with a minimum salinity value of just below 29 psu reached around Day 133, about 2 days after the peak of the wind stress. The local effect of the wind-induced freshwater burst lasts for about ten days, after which time the salinity reverts back to its earlier level.

In both the model and data, the freshwater event occurred just after a neap tide during which there was a northwest wind over the Strait of Georgia. For these two events, the salinity at Race Rocks decreased by about 2 psu, for a period of approximately ten days, in agreement with the model results. Minimum salinity is reached about two days after the minimum neap tide in both model and data.

To verify the importance of the timing of the neap tide and the wind burst, the experiment described above was repeated, but this time with the wind stress reaching a

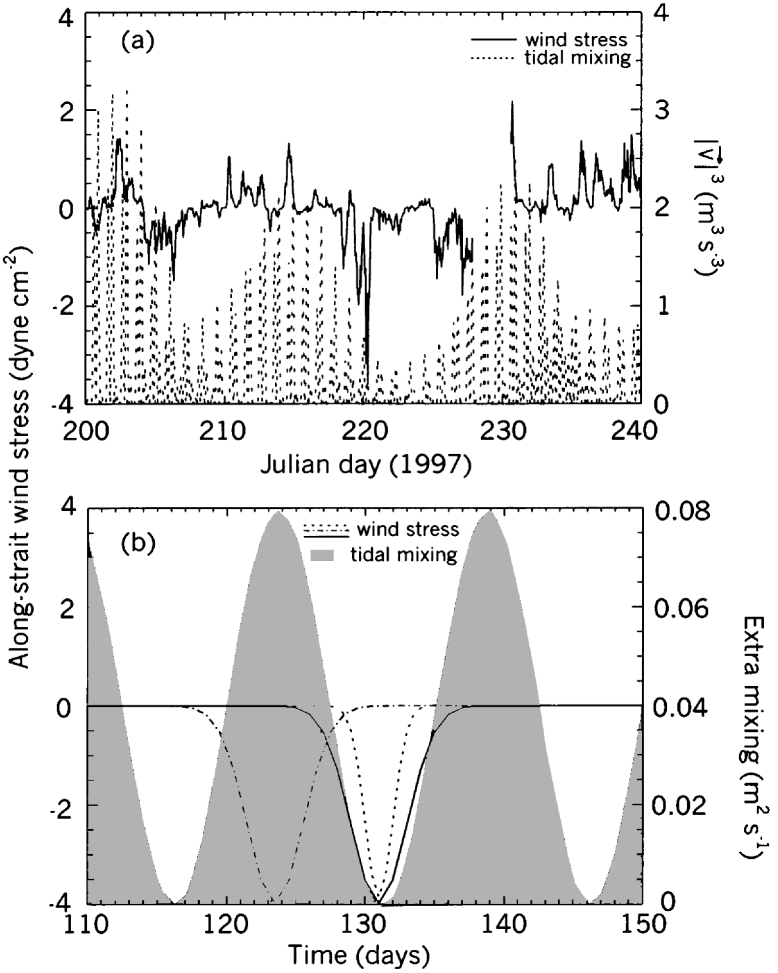

Figure 9. Wind stress, tidal mixing, and surface salinity during a strong freshwater pulse, from observations (a and c) and as obtained from the model (b and d). Surface salinity at Race Rocks is given for events observed in the summer of 1984 and 1997 (c), and from the model (d). In (c) the 40-day time series starts on June 29 and July 19 for 1984 and 1997, respectively. In (d), 5 cases are presented: (1) moderate wind at neap tide (solid line), (2) strong wind at neap tide (long dashed line), (3) weaker wind at neap tide (short dashed line), (4) shorter wind pulse (dotted line), and (5) moderate wind at spring tide (dashed-dotted line).

maximum during the preceeding spring tide, around Day 124 (Fig. 9b). The resulting Race Rocks salinity is included in Figure 9d, and shows no sign of a strong freshwater pulse in the area. In this case, the freshwater reaching Boundary Pass is prevented from flowing freely over the sill by the strong mixing associated with the spring tide. By the time the next neap is reached, the wind effect has vanished and the river plume in the Strait of Georgia has returned back to its position in the absence of wind. Also included in the figure are the

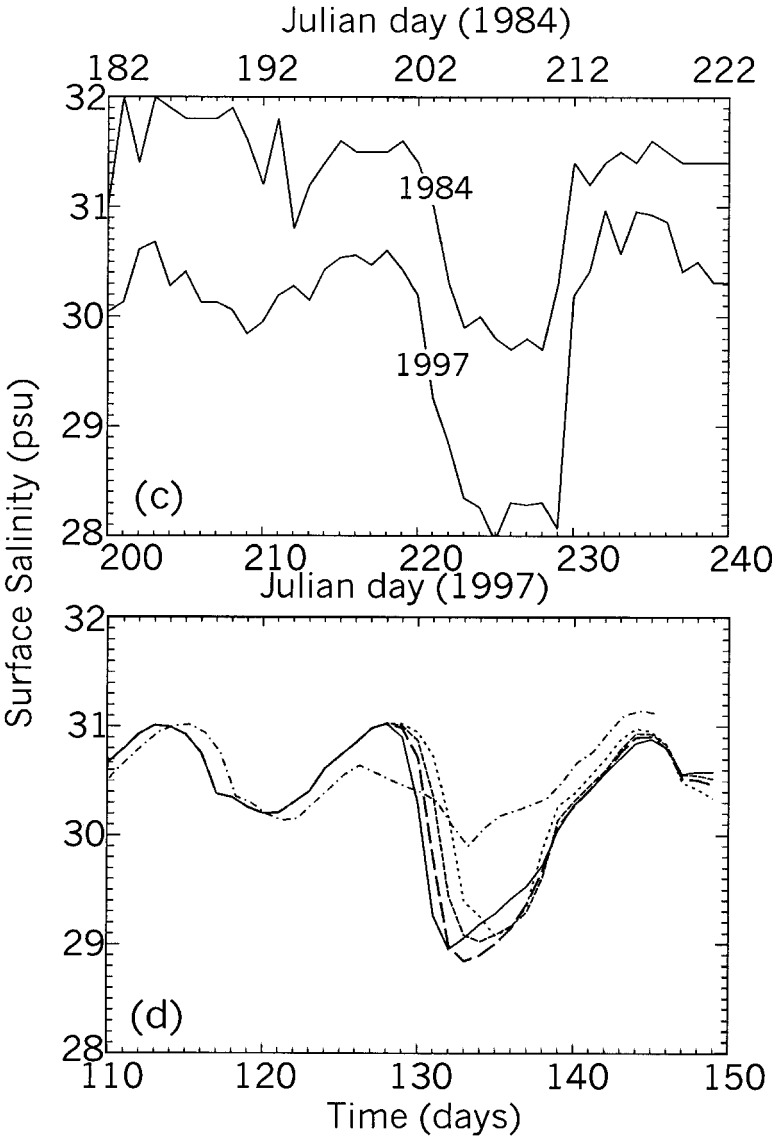

Figure 9. (Continued)

cases in which the wind stress amplitude was double and half of the first case as well as a case with a shorter wind pulse. The salinity obtained at Race Rocks is similar in all these cases, indicating that the strength of the wind or the duration of the pulse is not, within the tested range, critical in forming the freshwater pulse.

The freshwater pulses propagate seaward along the Canadian shore of Juan de Fuca Strait. A close examination of the modeled sea-surface elevation indicates that the wind

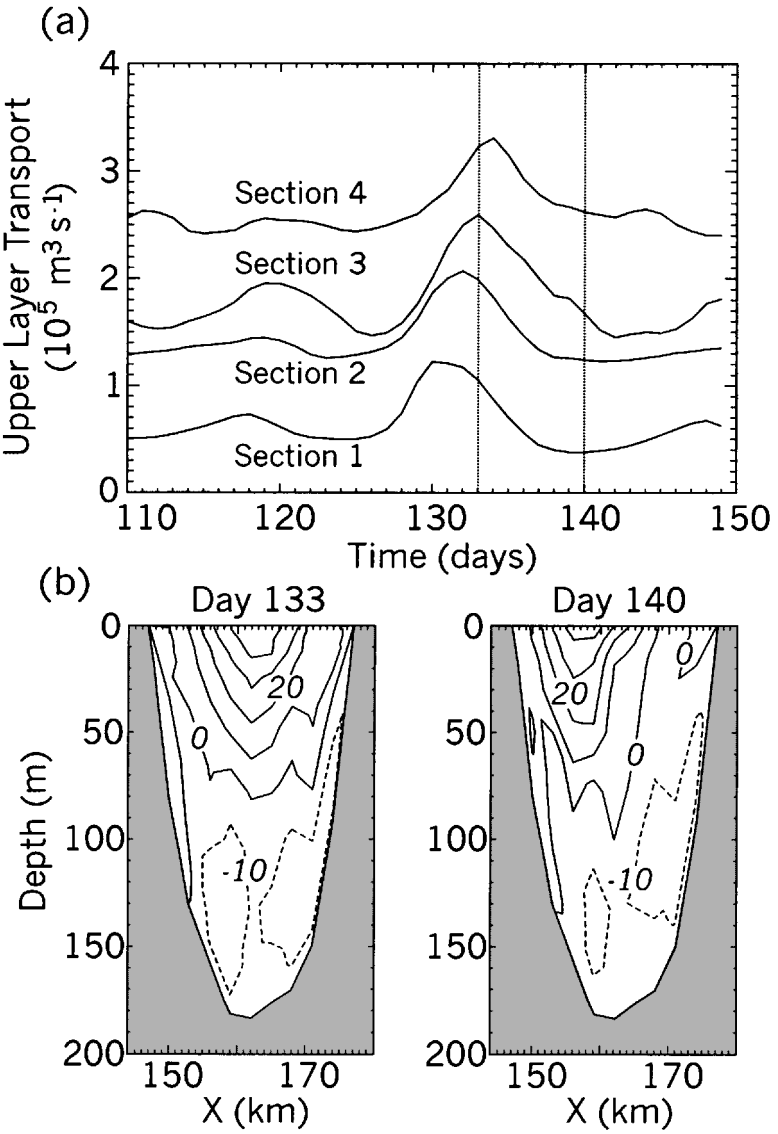

Figure 10. Effect of a wind-induced freshwater pulse on (a) the upper layer volume transport, and (b) the along-strait velocity contours in Juan de Fuca Strait. The locations of sections 1–4 are indicated on Figure 2. In (b), the velocity contours on section 3 are given at two times. The contour interval is 10 cm s^{-1}.

burst generates a signal that moves toward the mouth of the strait at a speed of about 50 km day^{-1} and that the associated surface displacement is maximum along the northern shore and decreases to zero within about 10 km of the coastal boundary. Figure 10 illustrates the impact of a large freshwater pulse on the circulation in Juan de Fuca Strait. In Figure 10a,

the volume transport of the upper layer across four sections of the strait is presented (see Fig. 2 for section locations) for the case described above in which a moderate wind burst reaches maximum amplitude during neap tides. About three days are required for the peak in volume transport associated with the freshwater pulse to travel from section 1 in Haro Strait to Section 4 at the mouth of Juan de Fuca, corresponding to a speed of advance of about 45 km/day. Also included in the figure are contours of the velocity component normal to section 3, midway along the strait, during and after passage of the pulse (Fig. 10b). At Day 133, the time of the maximum freshwater export through this section, the upper outflow is stronger and extends well across the strait to the Canadian coast, to a depth of about 80 m. On the other hand, 7 days later when the effect of the pulse has subsided, the velocity profile returns to its previous pattern, where the upper outflow is on the Washington side of the strait and the deeper inflow mostly on the B.C. side.

These characteristics correspond closely to those of a first mode internal Kelvin wave traveling along the north shore of the strait. Solution of the vertical eigenvalue problem (e.g., LeBlond and Mysak, 1978, section 24) based on a density profile from the middle of the strait yields an internal Rossby radius of 5.5 km for the first mode, with a zero-crossing depth of 70 m for the horizontal velocity, and a speed of propagation of 52 km/day. It thus appears that the wind burst generates a peak in upper layer transport that travels seaward trapped along the northern side of Juan de Fuca Strait as a first mode internal Kelvin wave. The horizontal resolution of 3 km used in the basic experiment would appear to be barely sufficient to resolve such a wave properly. However, results from the fine resolution experiment using a 1.5 km grid are similar to the ones from the basic case.

Following the passage of the initial Kelvin wave comes the actual pulse of fresher water, advected by the slower background estuarine surface outflow at about 20 km/day. Thus, the passage of a wind-induced freshwater pulse manifests itself first by a maximum value of upper layer transport (as well as surface velocity), followed by a minimum in surface salinity. Griffin and LeBlond (1990) observed in the 1984 data a similar time lag between maximum surface current and maximum temperature associated with the passage of a warm freshwater pulse at the site of a current meter mooring located near the estuary mouth.

5. Effects over the shelf

The preceeding sections demonstrate that the fortnightly modulation induced by tidal mixing is an important aspect of the summer dynamics of southern Georgia and eastern Juan de Fuca straits. The fortnightly signal was also shown to attenuate rapidly as it propagates downstream toward the shelf, in the western section of Juan de Fuca Strait. It has been suggested by Griffin and LeBlond (1990) as well as by Hickey *et al.* (1991) that such a modulation would strongly control the freshwater export onto the shelf and, therefore, the dynamics of the buoyancy-driven coastal current. However, evidence for such an effect has proven difficult to obtain as the velocity variance on the shelf is

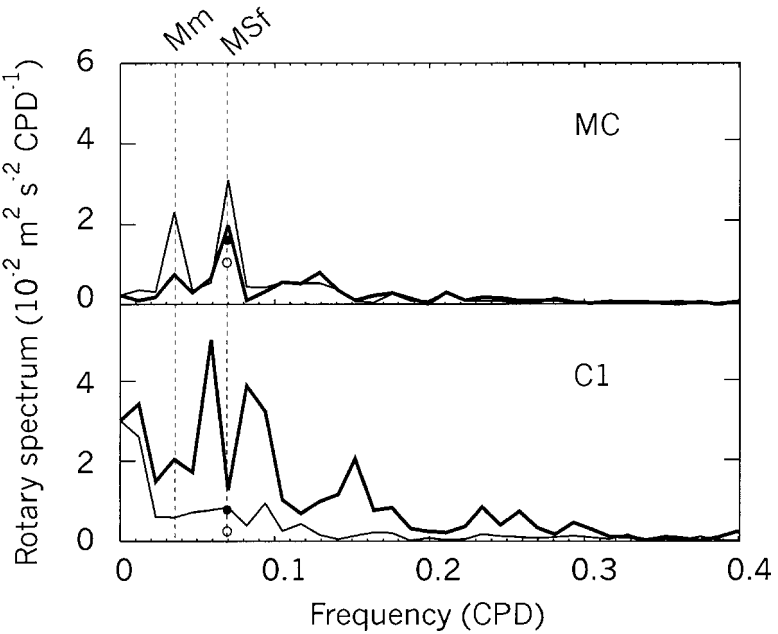

Figure 11. Rotary spectra for summer currents measured at a depth of about 30 m from current meter moorings located in eastern Juan de Fuca (MC of Fig. 1), and on the shelf (C1 of Fig. 1). Thick (thin) lines are for counterclockwise (clockwise) motions. Also shown are results of the basic experiment for the same locations (● for counterclockwise, ○ for clockwise). The monthly, Mm, and fortnightly, MSf, 'shallow water' tidal frequencies are indicated.

dominated by wind-driven variability generated both locally and remotely (Hickey *et al.,* 1991).

To examine the problem, rotary spectra of velocity measured at a depth of about 30 m are given in Figure 11 for both a shelf location (C1 on Fig. 1), and for a mooring inside the estuary (MC on Fig. 1). Mooring C1 is part of the ongoing La Pérouse Project (Thomson and Ware, 1996) and is located in 150 m of water, about 50 km west of the mouth of Juan de Fuca. The estuarine mooring, MC, a component of an ongoing monitoring program supported by the Capital Regional District of Victoria and the Institute of Ocean Sciences, was deployed off Macaulay Point in eastern Juan de Fuca, just downstream from the Victoria Sill. The spectra are an average based on several years of summer data (May to September): three years (1991 1993 and 1996) for MC, and two years for C1 (1985 and 1989).

The difference between the two spectra is striking. The low frequency variance of the Juan de Fuca mooring is dominated by peaks at the two 'shallow water' tidal frequencies Mm (27.55 day period) and Msf (14.76 day period). The reason for the two peaks is that during some periods, the two monthly neaps are approximately equal and the signal appears fortnightly, while at other times one neap dominates and the resulting signal

appears monthly. Mm and Msf are well known shallow water tidal constituents, due mostly to nonlinear interactions with topography and are expected to be present within the estuary. However, Griffin and LeBlond (1990) demonstrate convincingly that the signal in the waters off Victoria, as depicted in Figure 11, is stronger than one expected from shallow water tides alone, and is largely due to the fortnightly modulation of the tidal mixing. To confirm this idea, the rotary spectra were also estimated at MC for the winter periods and were found to be significantly (about 50%) less energetic. Such a seasonality could not be explained by a shallow water tidal phenomenon.

On the other hand, the generally red low frequency spectra of the shelf mooring (C1) reflects the importance of the regional wind-driven forcing typical of the shelf region, as found by Hickey *et al.* (1991). Evident in Figure 11 is the generally higher level of variance over the shelf relative to the estuarine location, reflecting the higher level of energy associated with large-scale atmospherically forced variability.

Figure 11 also includes results of the basic experiment for the same two locations. For MC, the estuarine location, the model gives spectral values of the fortnightly signal similar to the observed ones. The somewhat larger measured values could be the result of contributions from the shallow water tides which are not represented in the model. In the case of the shelf location, the model indicates small energy levels at the fortnightly frequency associated with small amplitude coastally trapped waves generated at the mouth of the estuary. Such a signal is almost certainly too weak to be detectable within the energetic shelf environment, as represented by the measured spectrum at C1. We thus conclude that the strong signal found in eastern Juan de Fuca Strait due to the fortnightly modulation of the tidal mixing is unlikely to lead to a significant modulation of the circulation on the shelf.

6. Conclusion

By combining model simulations with an analysis of data, this study has examined the influence of the fortnightly modulated mixing on the estuarine circulation in Juan de Fuca Strait, and on the export of freshwater onto the shelf. A version of the Princeton Ocean Model was used which includes riverine discharge, and an imposed fortnightly variation of the mixing over shallow sills inside the estuary. The model is initialized in a dam-breaking configuration, with fresher water within the estuary. A constant river discharge into the Strait of Georgia simulates the Fraser River outflow during summer. Following an adjustment period of about 40 days duration, the model produces a salinity field and an estuarine circulation which are in reasonable agreement with summer observations, with a realistic value for the layer volume transport of the order of 1.5 to 2×10^5 m^3 s^{-1}.

Forced by the modulation of the mixing over the sills, the modeled salinity within eastern Juan de Fuca Strait follows a marked fortnightly cycle of amplitude comparable to the observed one, with fresher water at the surface and saltier near the bottom during neap tides. However, the spring/neap salinity variability is largely confined to the eastern part of the strait, near the sill areas, with a much reduced signal at the mouth of the estuary. The

modeled estuarine transport has a moderate fortnightly component of about 20% of the mean near the mouth of the strait. Consequently, although the transport is modulated by the locally intense mixing over the shallow sills, the overall estuarine circulation in Juan de Fuca Strait is not strongly controlled by this modulation.

The model was also employed to simulate those infrequent and more dramatic events when a much fresher pulse of surface water escapes into eastern Juan de Fuca. In accordance with Griffin and LeBlond (1990), our results indicate that three conditions must be met for such large pulses to occur: a strong river discharge, low neap tidal velocities, and a concomitant northwesterly wind blowing over the Strait of Georgia. The model results showed relatively little sensitivity to the strength and the duration of the wind event. However, its timing relative to the neap tide is crucial to the formation of these stronger pulses.

The model results were also examined in terms of the effect of the fortnightly modulation of the buoyancy forcing on the circulation over the shelf. As observed in current meter data, the strong fortnightly signal obtained in the model experiment over eastern Juan de Fuca Strait does not induce a significant fluctuation on the shelf. Coastal trapped waves of modest amplitude are generated at the mouth of the estuary, but it is unlikely that such a weak signal can be distinguished from the higher level of energy associated with large-scale wind forced variability typically found on the shelf.

In general, the present numerical model is successful in representing some features of the complex problem of modulated estuarine circulation studied here. The relative simplicity of the paramerization used to represent the tidally induced mixing allowed us to identify the effects of this process on the local dynamics. Such an approach could be extended in the future to study the implications of the fortnightly modulation of the tidal mixing on the dynamics inside the Strait of Georgia. For example, it could be used to examine the importance of such a process on the deep water renewal within the estuary which is vital to sustaining the local ecosystem.

Acknowledgments. We thank Lie-Yauw Oey for providing his version of the Princeton Ocean Model. Most of the current meter data used in this study were collected under the direction of R. E. Thomson. Tidal velocities were gracefully provided by Mike Foreman. We also thank the referees for their constructive comments.

REFERENCES

Birch, J. R. 1991. Deep water renewal at neap tides in the southern Strait of Georgia, 1989–1990. Unpub. Rep. by Arctic Sciences Ltd. Sidney, B.C. for the Institute of Ocean Sciences, 43 pp.

Blumberg, A. F. and G. L. Mellor. 1987. A description of a three-dimensional coastal ocean circulation model, *in* Three Dimensional Coastal Ocean Models, Coastal and Estuarine Science Series, Vol. 4, N. Heaps Ed., Amer. Geophys. Union, 1–16.

Crean, P. B. and A. B. Ages. 1971. Oceanographic records from twelve cruises in the Strait of Georgia and Juan de Fuca Strait, 1968. Department of Energy, Mines, and Resources, Marine Research Sciences Branch, Vol. 1–4, 389 pp.

Farmer, D. M. and J. D. Smith. 1980. Tidal interaction of stratified flow with a sill in Knight Inlet. Deep-Sea Res., *27A,* 239–254.

Foreman, M. G. G., R. A. Walters, R. F. Henry, C. P. Keller and A. G. Dolling. 1995. A tidal model for eastern Juan de Fuca Strait and the southern Strait of Georgia. J. Geophys. Res., *100* C1, 721–740.

Frisch, A. S., J. Holbrook and A. B. Ages. 1981. Observations of a summertime reversal in circulation in the Strait of Juan de Fuca. J. Geophys. Res., *86* (C3), 2044–2048.

Geyer, W. R. and G. A. Cannon. 1982. Still processes related to deep water renewal in a fjord. J. Geophys. Res., *87* C10, 7985–7996.

Geyer, W. R. and H. Nepf. 1996. Tidal pumping of salt in a stratified estuary. Coast. Estuar. Stud., *53,* 213–226.

Godin, G., J. Candela and R. de la Paz-Vela. 1981. An analysis and interpretation of the current data collected in the Strait of Juan de Fuca in 1973, 1981. Mar. Geodesy, *5,* 273–302.

Griffin, D. A. and P. H. LeBlond. 1990. Estuary/ocean exchange controlled by spring-neap tidal mixing. Estuar. Coast. Shelf Sci., *30,* 275–297.

Herlinveaux, R. H. and J. P. Tully. 1961. Some oceanographic features of Juan de Fuca Strait. J. Fish. Res. Bd. Canada, *18,* 1027–1071.

Hibiya, T., M. Ogasawara and Y. Niwa. 1998. A numerical study of the fortnightly modulation of basin-ocean water exchange across a tidal mixing zone. J. Phys. Oceanogr., *28,* 1224–1235.

Hickey, B. M., R. E. Thomson, H. Yih and P. H. LeBlond. 1991. Velocity and temperature fluctuations in a buoyancy-driven current off Vancouver Island. J. Geophys. Res., *96,* 10507–10538.

Holbrook, J. R., R. D. Muench, D. G. Kachel and C. Wright. 1980. Circulation in the Strait of Juan de Fuca. NOAA Technical Report, ERL 412-PMEL 33, 42 pp.

Labrecque, A. J. M., R. E. Thomson, M. W. Stacey and J. R. Buckley. 1994. Residual currents in Juan de Fuca Strait. Atmos. Ocean, *32,* 375–394.

LeBlond, P. H., D. A. Griffin and R. E. Thomson. 1994. Surface salinity variations in the Juan de Fuca Strait: test of a predictive model. Cont. Shelf Res., *14,* 37–56.

LeBlond, P. H. and L. A. Mysak. 1978. Waves in the Ocean, Elsevier Sci., NY, 602 pp.

Masson, D. and P. F. Cummins. 1999. Numerical simulations of a buoyancy-driven coastal countercurrent off Vancouver Island. J. Phys. Oceanogr., *29,* 418–435.

Mellor, G. L. and T. Yamada. 1982. Development of a turbulent closure model for geophysical fluid problems. Rev. Geophys. Space Phys., *20,* 851–875.

Oey, L. Y. 1996. Simulation of mesoscale variability in the Gulf of Mexico: Sensitivity studies, comparison with observations, and trapped wave propagation. J. Phys. Oceanogr., *26,* 145–175.

Oey, L. Y. and P. Chen. 1992. A model simulation of circulation in the northeast Atlantic shelves and seas. J. Geophys. Res., *97,* 20087–20115.

Oey, L. Y. and G. L. Mellor. 1993. Subtidal variability of estuarine outflow, plume, and coastal current: a model study. J. Phys. Oceanogr., *23,* 164–171.

Park, K. and A. Y. Kuo. 1996. Effect of variation in vertical mixing on residual circulation in narrow, weakly nonlinear estuaries. Coast. Estuar. Stud., *53,* 301–317.

Pawlowicz, R. and D. F. Farmer. 1998. Diagnosing vertical mixing in a two-layer exchange flow. J. Geophys. Res., *103,* 30695–30712.

Royer, L. and W. J. Emery. 1985. Computer simulations of the Fraser River plume. J. Mar. Res., *43,* 289–306.

Thomson, R. E., B. M. Hickey and P. H. LeBlond. 1989. The Vancouver Island coastal current: fisheries barrier and conduit, *in* Effects of Ocean Variability on Recruitment and an Evaluation of Parameters Used in Stock Assessment Models. Can. Spec. Publ. Fish. Aquat. Sci., *108,* 265–296.

Thomson, R. E. and D. M. Ware. 1996. A current velocity index of ocean variability. J. Geophys. Res., *101,* 14297–14310.

Received: *16 September, 1999;* revised: *9 March, 2000.*